

# Perception of surface slant from oriented textures

Jeffrey A. Saunders

Departments of Psychology, University of Pennsylvania,  
Philadelphia, PA, USA



Benjamin T. Backus

Departments of Psychology, University of Pennsylvania,  
Philadelphia, PA, USA



When a surface covered with a regular texture is viewed in perspective, the projected texture provides a number of cues to 3D surface orientation. For oriented textures, one cue is perspective convergence: symmetry lines that are parallel along the surface project to lines that vary systematically in orientation. We investigated the contribution of perspective convergence to perception of 3D slant and tested whether slant from convergence depends on oriented spectral components. Subjects judged the sign of slant about a vertical axis of rotation. Textures were composed of filled circles in three spatial arrangements: a hex grid with symmetry lines at 0 and  $\pm 60$  deg relative to the tilt direction (aligned condition), a hex grid with symmetry lines at 90 and  $\pm 30$  deg (perpendicular condition), and random arrangements with similar average spacing (isotropic condition). The two hex grid textures differed in the amount of spectral energy present in the tilt direction (horizontal) but were otherwise closely matched. Slant discrimination thresholds for monocular stimuli were higher for isotropic textures than for either of the two hex grid textures and were higher for the perpendicular texture than for the aligned texture. In a second experiment, we measured the weight given to texture relative to binocular slant information for cue conflict stimuli ( $\pm 5$  deg). Weights were found to agree with individual subjects' monocular thresholds, in accordance with optimal estimation theory. We conclude that the visual system uses perspective convergence to perceive slant and that effective use of convergence requires the presence of spectral components aligned with the tilt direction.

Keywords: texture gradients, slant perception, depth perception, linear perspective, cue integration, 3D vision

## Introduction

Visual texture can be a powerful cue to the 3D structure of surfaces. When a surface with a regular texture is viewed in perspective, the projected texture varies across the image as a function of the slant or curvature of the surface. Gibson (1950) pointed out the potential information provided by visual texture and introduced the term *texture gradient* to refer to such variations. There is now a considerable body of work studying the role of texture in human vision, for perceiving both the 3D shape of curved surfaces (e.g., Cumming, Johnston, & Parker, 1993; Li & Zaidi, 2000, 2001, 2003; Todd & Akerstrom, 1987; Todd & Oomes, 2002; Todd, Oomes, Koenderink, & Kappers, 2004) and the 3D orientation of planar surfaces (e.g., Andersen, Braunstein, & Saidpour, 1998; Beck, 1960; Buckley, Frisby, & Blake, 1996; Knill, 1998a, 1998b; Passmore & Johnston, 1995; Rosas, Wichmann, & Wagemans, 2004; Saunders, 2003; Todd, Thaler, & Dijkstra, 2005). Texture has also been studied as a 3D cue in the area of computational and computer vision (Aloimonos & Swain, 1988; Blostein & Ahuja, 1989; Gårding, 1993; Ikeuchi, 1984; Knill, 1998c; Sakai & Finkel, 1995, 1997; Stevens, 1981b; Super & Bovik, 1995; Turner, Gerstein, & Bajcsy, 1991; Witkin, 1981).

Understanding how texture gradients are used perceptually is complicated by the fact that they generally contain a number of different regularities that could be exploited to compute slant and shape, corresponding to

different constraints that could apply to the surface texture. Figure 1 shows an example of a texture gradient and a number of potential texture cues. Decompositions of texture gradients into different components have been put forth by a number of researchers (Blake, Bulthoff, & Sheinberg, 1993; Cutting & Millard, 1984; Knill, 1998a; Saunders, 2003).

When a texture has one or more dominant orientations, a cue that becomes available is *perspective convergence*. In the example shown in Figure 1, dominant orientations result from the symmetric arrangement of elements, which are organized into regular rows and diagonals. These symmetry lines are parallel along the surface, but due to perspective, their projections vary in orientation, converging toward a point on the horizon associated with the surface. As illustrated in Figure 2, there is a simple mathematical relation between the direction and amount of convergence in an image and the 3D slant and tilt of the surface<sup>1</sup> (see also Saunders & Knill, 2001). In these examples, the textures are highly regular, but textures can also have dominant orientations in a more statistical sense. To provide a perspective convergence cue, it suffices that a texture has some anisotropy that is homogeneous across the surface, such as that of wood grain.

The experiments reported here investigate the use of perspective convergence for perception of 3D surface slant. We had two aims: (1) to assess the effectiveness of convergence as a cue to slant relative to other texture cues and (2) to examine whether the visual system measures

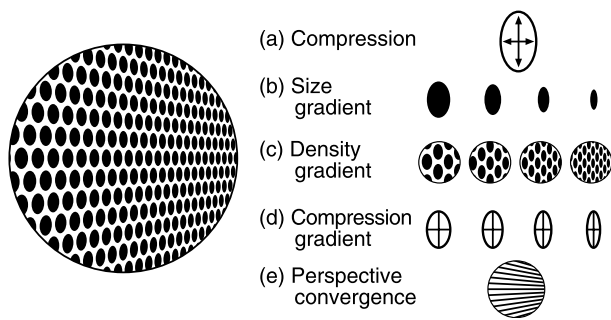


Figure 1. Some regularities that provide information about the 3D orientation of the textured surface relative to the line of sight. (a) If texture elements are circular, then the aspect ratios of their projected contours indicate local slant—a compression cue. (b) If texture elements have uniform size along a planar surface, then the gradient of their projected sizes specifies slant—a size gradient cue. (c,d) Analogous density and compression gradient cues. (e) If texture has oriented structure, then an additional cue that becomes available is perspective convergence. In this example, if the rows are assumed to be parallel along the surface, then their convergence in the projected image provides a cue to slant.

perspective convergence spectrally, from oriented spatial frequency components in an image.

## Previous psychophysical work

Previous studies have demonstrated that convergence can be an effective cue to 3D slant, at least in the case of ruled surfaces (Andersen et al., 1998; Gillam, 1968; Todd et al., 2005) that also contain a gradient of spatial frequency. However, the relative contribution of perspective convergence when other texture cues are present is not well established. Much of the previous work on slant from texture used isotropic textures, for which perspective convergence is absent (e.g., Buckley et al., 1996; Knill, 1998c; Knill & Saunders, 2003; Saunders, 2003). Rosas et al. (2004) and Todd et al. (2005) studied both isotropic textures and textures with oriented structure (gratings, plaids, and grids) that would produce perspective convergence. Rosas et al. observed no advantage in slant discrimination performance for plaid or grid textures in comparison with the best instances of isotropic textures. On the other hand, Todd et al. did observe a reliable improvement in accuracy of slant judgments for plaid and grating textures over isotropic textures, particularly for small-to-moderate fields of view.

Two studies put perspective convergence into conflict with other texture information—specifically, with texture compression. Braunstein and Payne (1969) tested rectangular grid textures that had different ratios between row and column spacing, which changes the projected aspect ratios, or “form ratios,” of the individual rectangles. Slant judgments were found to depend primarily on perspective con-

vergence. Tibau, Willems, Van den Bergh, and Wagemans (2001) tested a similar class of grid textures, in which local compression and perspective convergence were independently varied, and also found a strong influence of perspective. However, in both these studies, convergence was confounded with other gradient cues, including the compression gradient, which has been observed to be an effective texture cue in isolation (Andersen et al., 1998).

Locally parallel contours along surfaces have also been studied as a basis for perceiving the 3D shape of curved surfaces (Knill, 2001; Stevens, 1981a; Todd & Reichel, 1990). The problem of computing shape from surface contours is similar to computing slant from perspective convergence, in that both involve using the pattern of orientations in a projected image to infer 3D structure, based on a parallelism assumption. However, there may be differences in how image orientations are used. In particular, shape from surface contours can be effective even if projection is orthographic rather than perspective, and previous studies have mostly used orthographic projections for stimuli. For planar surfaces, perspective projection is required for oriented symmetries to provide information because, under orthographic projection, parallel lines remain parallel.

One goal of our experiments was to provide a strong test of whether perspective convergence contributes to perceived slant when other texture cues are present. We did this by comparing performance for highly regular textures that were matched for their size, density, and compression gradients, as well as for local compression (texture element aspect ratio), but differed in the presence and/or the alignment of

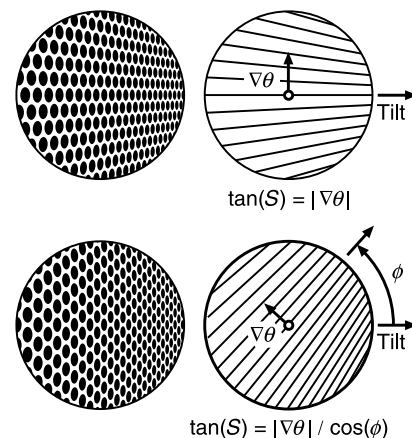


Figure 2. Perspective convergence and 3D surface orientation. The left panels show views of slanted surfaces with textures that contain oriented symmetries. The right panels show one set of symmetry lines for illustration. The convergence can be described by the gradient of line orientation in the image ( $\nabla\theta$ ). In the top panels, symmetry lines are aligned with the surface tilt direction. In this case, the magnitude of the orientation gradient is equal to the tangent of surface slant. In the bottom panels, symmetry lines are not aligned with the tilt direction, but the orientation gradient still constrains the possible slant and tilt of the surface.

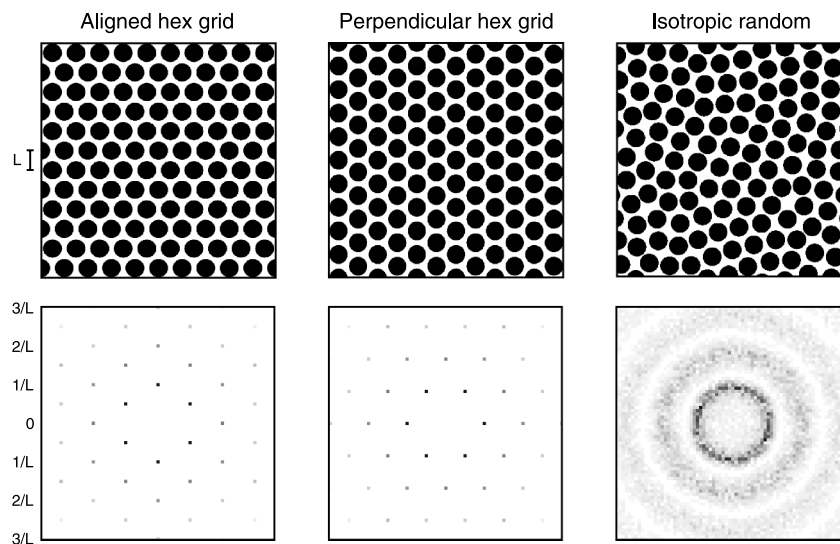


Figure 3. The three textures used in the experiments. The top row shows the textures, and the bottom row shows a portion of their 2D discrete Fourier transforms (amplitude spectra). All three textures were composed of uniformly sized circular elements and differed only in the arrangement of the elements. For the isotropic random texture (right), random initial positions were chosen and an iterative repulsion process was applied to increase the regularity of spacing. The spectrum does not have an orientation but is, instead, composed of circular rings. For the aligned hex grid (left), elements were arranged on a hex grid in which the main directions of symmetry were 0 and  $\pm 60$  deg relative to horizontal. The spectrum contains isolated peaks arranged in a hex lattice. The perpendicular hex grid (middle) was the same as the aligned hex grid except that the pattern was rotated by 90 deg (or equivalently, by 30 deg). The spectrum is also a hex grid, but compared to the aligned texture, there is less contrast energy in the horizontal direction, at higher spatial frequencies. This difference may be a factor in why the aligned texture organizes perceptually into horizontal rows (plus diagonals), whereas the perpendicular texture organizes into vertical columns (plus diagonals), and why perspective convergence is a more effective slant cue for the aligned texture (see results).

their oriented symmetries. Samples are shown in Figure 3. The textures were composed of discrete circular disks of uniform size. This class of textures would, in principle, allow easy image measurements of local compression and the gradients of size and spacing, based either on individual texture element features (e.g., Blostein & Ahuja, 1989; Witkin, 1981) or on local spectral encodings (e.g., Gårding, 1993; Sakai & Finkel, 1995, 1997).

Previous studies using isotropic textures found texture compression to be the main determinant of perceived slant (Buckley et al., 1996; Knill, 1998c; Rosenholtz & Malik, 1997; Saunders, 2003), and the results of Braunstein and Payne (1969) suggest that compression can dominate perspective information when these cues are in conflict. We therefore focused on the case of surfaces with low slant (i.e., surfaces that are nearly frontal). Texture compression is mathematically least informative in this case (Knill, 1998a). This choice also makes sense in light of the results of Andersen et al. (1998), which suggest that convergence (by itself) is a more effective slant cue than compression at low slants but is less effective at high slants.

### Spectral models of shape from texture

How might perspective convergence be measured and used? Li and Zaidi (2000) proposed that perception of shape from texture is based on patterns of orientations in

an image, measured using peaks of energy in the spectral domain. If a dominant orientation in a texture corresponds to an identifiable peak in its Fourier spectrum, then perspective convergence in an image can be measured from changes across space in the local spectra of the projected texture. Figure 4 shows examples of local spectra for an image that contains perspective convergence. The spectra from the upper and lower regions of the image have energy peaks at different orientations, thereby providing a mea-

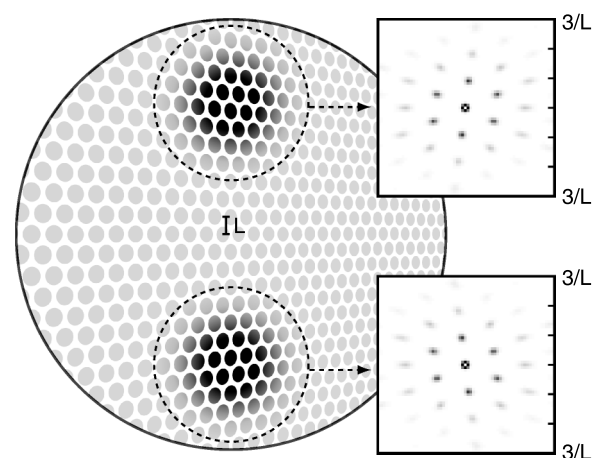


Figure 4. Illustration of the local spectra (right) for two different regions of an image (dashed circles).

sure of perspective convergence. This is consistent with using an initial stage of Gabor-like filters as input to computing slant from convergence, as in the model of Super and Bovik (1995).

Recent computer vision models generally presuppose spectral descriptions of texture, treating surface markings as being 2D reflectance patterns rather than as a distribution of individual elements. This is advantageous because some natural textures cannot be easily described in terms of individual elements (e.g., tree bark, rough plaster), and even if texture elements are well defined, isolating and measuring projected elements within an image could pose difficulties. Additionally, a spectral-based (or wavelet-based) representation would be consistent with visual coding in early stages of human visual processing (Watson & Ahumada, 2005).

Several proposed models use variations in local spectra across a projected image to infer 3D structure, under the assumption that the surface texture is homogenous. Super and Bovik (1995) and Turner et al. (1991) assume that a texture has some dominant spatial frequency component that is uniform across a surface and use the dominant spatial frequencies and orientations in local image regions to infer surface orientation. These models make use of both perspective convergence and the gradient in texture scale. Sakai and Finkel (1995, 1997) similarly assume that surface texture has some dominant spatial frequency but not necessarily a uniform orientation; hence, they used changes in mean spatial frequency across an image, rather than both frequency and orientation. This is a spectral-domain analog to using just the size gradient of texture to compute slant. Malik and Rosenholtz (1997) propose a more general model based on an assumption of homogeneity, which attempts to compute affine mappings between local spectra in different regions of the image and which would not require a texture to have a dominant orientation or spatial scale. A different approach proposed by Gårding (1993) uses anisotropy in local spectra to infer local surface orientation, under the assumption that the surface texture is isotropic. This is analogous to using local compression of texture elements as a cue (see Figure 1).

The oriented-energy model proposed by Li and Zaidi was motivated by their observations in a shape from texture task (Li & Zaidi, 2000). Subjects judged the relative depths of neighboring points along sinusoidally corrugated textured surfaces, and a global perceived surface was inferred from the pairwise judgments. Surface textures were composed in the spectral domain (i.e., superimposed gratings, filtered noise), which allowed explicit control of the spectral components. Li and Zaidi found that the isotropic filtered-noise textures were not effective at supporting veridical shape perception for their task and conditions: These surfaces appeared compressed in depth (and were also rectified inconsistently). Performance for anisotropic textures was much better, provided that their spectra had a discrete energy component aligned with the direction of surface curvature (i.e., the local tilt direction). Li and Zaidi observed that, across a range of textures with dif-

ferent subjective appearances, the presence of an aligned spectral component was sufficient for reliable judgments of the qualitative shape. They concluded that oriented spectral energy was the essential factor for texture as a shape cue.

Although Li and Zaidi considered 3D shape rather than slant, their use of orientation modulations in perspective projections is essentially equivalent to using perspective convergence to infer local slant. Thus, their conclusions about the importance of oriented spectral energy could apply to the perception of planar slant as well.

To test whether oriented energy is important for perceiving slant from texture, we compared performance for the left and middle textures in Figure 3. These textures potentially provide the same perspective convergence information; in both cases, an ideal observer that identifies horizontal lines and measures the convergence of these lines in the image could easily be constructed. They are also closely matched with respect to other texture cues like size, spacing, and compression. However, the two textures contain different amounts of oriented spectral energy in the tilt direction (Figure 3, bottom panels). While the horizontal rows in the aligned textures correspond to peaks in spectral energy, the horizontal rows in the perpendicular texture do not. Thus, although the perpendicular texture contains clear horizontal lines, this structure is not reflected in the spectral (or wavelet) representation of orientations. We would therefore attribute any difference in the effectiveness of these textures at conveying slant to their difference in spectral representations and would take this as strong evidence for an oriented-energy model.

Figure 5 shows examples of slanted perspective views of surfaces with all three types of texture. The images along each row were generated with the same slant, but subjectively, there are clearly differences in the amount of apparent slant across texture types. The isotropic texture (right) is least effective at conveying slant. Although size, shape, and spacing are highly regular, it is hard to see this surface as slanted, even for a simulated slant as high as 20 deg. The aligned hex grid texture (left) produces a dramatically more salient percept of slant (as well as lower slant thresholds; see Experiment 1). This difference must be due to the presence of oriented symmetries because the isotropic and hex grid textures are closely matched otherwise. The perpendicular hex grid texture (middle), for which most spectral energy is at vertical or diagonal orientations, is an especially interesting case. This texture is more effective at conveying slant than the isotropic texture but less effective than the aligned hex grid texture. The horizontal symmetries in the perpendicular hex grid texture could easily be measured by a mechanism designed to detect them, given the high regularity of the pattern. However, when symmetries do not correspond to large amounts of energy in the spectral domain, they are not very effective at eliciting perceived slant.

The two experiments presented here quantify the effects visible in Figure 5. In Experiment 1, we measured slant discrimination thresholds for the three different types of

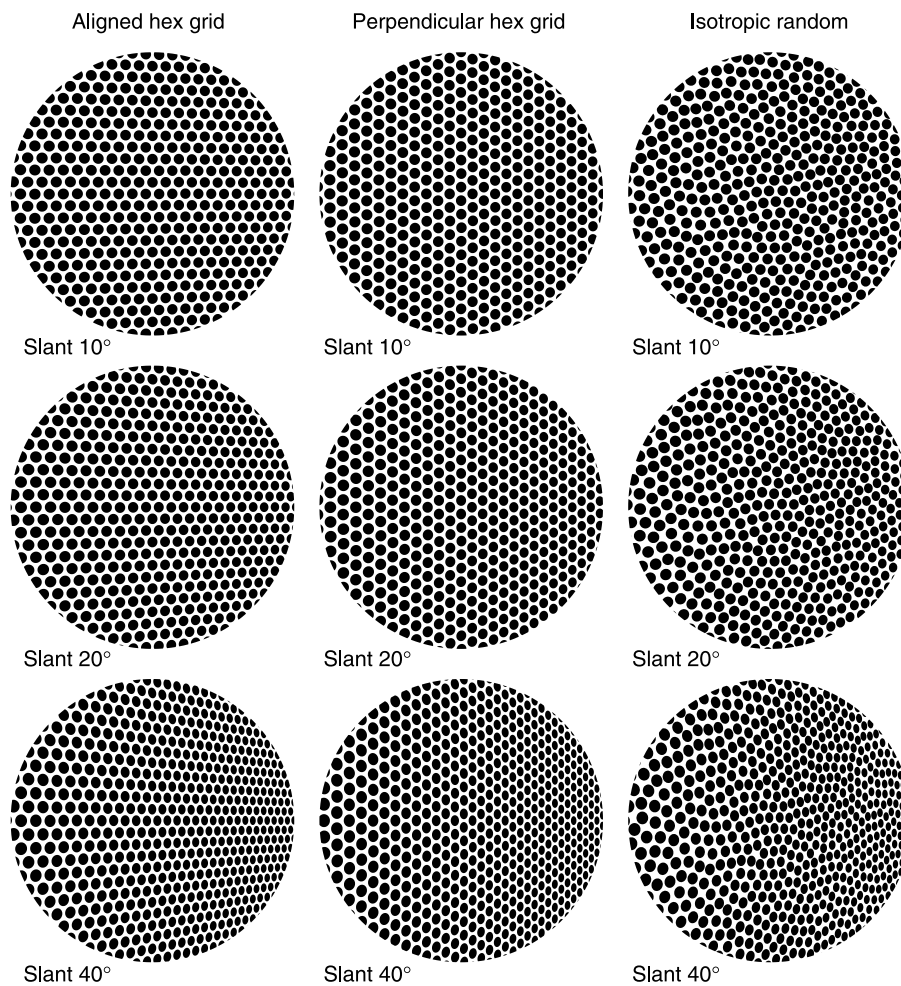


Figure 5. Examples of texture stimuli. In the experiments, the circular apertures subtended 30 deg of visual angle. The three columns show the aligned hex grid, the perpendicular hex grid, and the isotropic random texture. The simulated slant in each row is 10, 20, and 40 deg, respectively. Slant discrimination thresholds were lowest for the aligned hex grid (left), next lowest for the perpendicular grid (center), and highest for the isotropic random texture (right).

texture. Thresholds showed large differences across texture types, in the direction expected based on their subjective appearances. In [Experiment 2](#), we measured the relative contributions of texture and stereo slant information for cue conflict stimuli. If these sources of information were integrated optimally, as observed previously (Hillis, Watt, Landy, & Banks, 2004; Knill & Saunders, 2003), one would expect the visual system to give greater weight to textures that produce better discrimination performance. The results confirmed this prediction.

## Experiment 1

### Methods

#### *Apparatus and display*

The stimuli were computer-generated perspective images of slanted planar surfaces covered with texture, as viewed

through a 30-deg-diameter blurred aperture. The images were presented with a haploscope, consisting of two Clinton monochrome CRT monitors, each seen through a mirror by one eye. The mirrors were approximately  $6 \times 10$  cm, rounded in shape to fit close to the eyes, and were oriented at 45 deg relative to the line of sight. The monitors had a resolution of  $1,280 \times 1,024$  pixels and a refresh rate of 75 Hz and were positioned so that their images through the mirror were both frontal relative to the cyclopean line of sight and at an optical distance of 40 cm. In [Experiment 1](#), images were viewed monocularly: Subjects wore a patch over their left eye, and simulated surfaces were centered in front of their right eye. The haploscope apparatus was therefore unnecessary for this experiment but was used so that displays would be consistent with those of [Experiment 2](#), which did make use of the stereo display capability.

The haploscope's mirrors were half-silvered to allow optically based spatial calibration, which was necessary to compensate for curvature of the display monitors. During the calibration procedure, the experimenter adjusted the po-

sitions of a grid of visual points presented on the display to match a precisely calibrated physical grid viewed through the half-silvered mirror. This matching was done separately for each eye's view. The mappings between corresponding pairs of world and pixel coordinates were fit by sixth-degree 2D polynomials, which were applied to world coordinates when generating images. Images were rendered using OpenGL, and all simulated objects were antialiased with sub-pixel resolution.

The simulated surface textures were composed of 0.8-cm-diameter dots ( $\sim 1.1$  deg) on a darker background. There were three texture type conditions, corresponding to the examples shown in [Figure 3](#). For the *aligned* texture, dots were centered at points of a hexagon grid, with a center-to-center spacing of 1 cm ( $\sim 1.4$  deg). The *perpendicular* texture was identical to the aligned texture, except for it being rotated 90 deg within its plane. For the *isotropic* textures, dot positions were determined by starting with a random sample drawn from a uniform distribution and then applying an iterative procedure to increase the uniformity of spacing to make uniformity of spacing similar to that of the two hex grid textures. This procedure consisted of simulating mutual repulsion between elements and iterating until the configuration stabilized. Opposite edges of the square region were treated as being connected (i.e., elements distributed on a torus) so that the resulting configuration would tile. The magnitude of simulated repulsion decreased as a Gaussian function of distance, with Gaussian width equal to half of the distance between neighboring points in a hex arrangement with the same area and density. Ten different texture samples were generated by this procedure, each with 256 points within a  $14.9 \times 14.9$  cm square region ( $\sim 21 \times 21$  deg). On each trial in the isotropic condition, one sample from this set was randomly chosen and tiled to extend throughout the surface. The isotropic textures were also randomly rotated and translated on each trial to add further variability. Random translations were also added to the hex grid textures.

### Procedure

Four subjects participated in [Experiment 1](#). All had normal or corrected-to-normal vision. One subject (J.A.S.) was the first author. The other subjects were naive to the purposes of the experiment. All subjects gave informed consent in accordance with a protocol approved by the human subjects Institutional Review Board of the University of Pennsylvania.

Subjects performed four blocks of 180 trials, on 4 separate days, yielding 240 trials per texture condition for each subject. The three textures were randomly intermixed within blocks. In each session, subjects also performed a block of slant discrimination trials for stereo stimuli, the results of which are reported in [Experiment 2](#). The order of presentation for the monocular and stereo blocks was counterbalanced across sessions and subjects.

On each trial, a stimulus image was presented for 1 s, followed by a mask consisting of binary pixel noise. The task of the subjects was to judge the sign of slant of the

textured surfaces—that is, whether the left or right side of the surface was closer. After initial instruction, subjects received no feedback. They were instructed to fixate a small (0.2 deg) fixation marker that was visible throughout the experiment.

Simulated slant was varied across trials for a given texture using a new adaptive procedure, as described in [Appendix A](#). The set of responses was used to compute maximum likelihood estimates of the point of subjective equality (PSE) and 75% threshold. The PSE represents constant bias in perceived slant. The threshold was of main interest in this experiment, representing subjects' ability to discriminate the sign of slant. A cumulative Gaussian was used to model the psychometric function. The "mean" parameter of the best fitting function was the PSE, and the difference between the mean and the 75% point was the discrimination threshold (this is 0.674 times the cumulative Gaussian's standard deviation parameter). Statistical comparisons between thresholds in different conditions were based on the likelihood functions computed to fit the data. To evaluate whether a threshold  $\sigma_1$  was reliably larger than another threshold  $\sigma_2$ , we assumed that the likelihood function for each condition represented the true probability of getting the observed results (as a function of possible threshold values) and computed from these the probability of the null hypothesis,  $\sigma_1 \leq \sigma_2$ .

### Results and discussion

The graphs in [Figure 6](#) plot discrimination thresholds for each of the three textures, for the four different subjects. Although subjects showed individual differences in overall performance, there was consistent rank order in the results: The aligned hex grid produced the lowest thresholds, followed by the perpendicular hex grid, with the isotropic texture producing the highest thresholds. We used the estimated likelihood functions computed when fitting the data to compute 95% confidence intervals (shown in [Figure 6](#)) and to carry out pairwise statistical comparisons. For all subjects, thresholds for the three texture types were all significantly different from one another ( $p < .01$ ).

By design, the textures were closely matched for compression and size cues; thus, differences in performance must be due to the arrangement of texture elements. Variability in density also cannot account for differences. The regularity in spacing was identical for the aligned and perpendicular textures and closely matched for isotropic textures. Moreover, other evidence suggests that density is a weak texture cue for isotropic textures (Buckley et al., 1996; Cutting & Millard, 1984; Knill, 1998b, 1998c; Stevens, 1981b). We conclude that the differences between texture types must be due to the oriented symmetries in the arrangements.

The better discrimination performance for the aligned texture relative to isotropic textures can be explained by use of perspective convergence as a slant cue. Previous work has

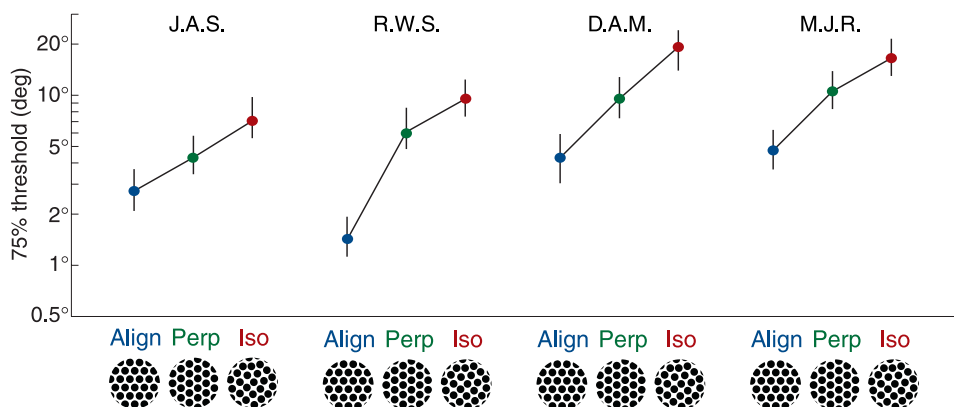


Figure 6. Seventy-five percent thresholds observed for the monocular stimuli in Experiment 1, for each subject and texture type. Error bars depict 95% confidence intervals.

shown that convergence can be an effective slant cue for minimal stimuli (Andersen et al., 1998; Todd et al., 2005). The present results show that, for the case of surfaces near the frontal plane, convergence is a strong determinant of perceived slant even when other potential texture cues are available.

Our aligned and isotropic textures are similar to textures used in a demonstration by Li and Zaidi (2004). They compared the perceived curvature of surfaces covered either with randomly positioned dots or with dots aligned on a rectangular grid (Figure 9 in Li & Zaidi, 2004). As in our experiment, the only difference was in the arrangement of dots. In Li and Zaidi’s demonstration, the grids are more effective at conveying the shape (concave vs. convex) than the dots that are randomly positioned, consistent with our results. We more closely matched the regularity of our isotropic textures and grid textures, but otherwise, the comparison is similar.

The difference we observed between aligned and perpendicular textures is striking because of their high degree of similarity. The two texture types are matched in terms of the size, shape, and spacing of the texture elements, and they share the same six directions of symmetry as well. In particular, both textures contain clearly defined rows (Figure 7a). This similarity is obscured by that fact that the rows in the aligned texture are more perceptually salient, but geometrically, there is little difference in the arrangements of element positions. In fact, the two arrangements can be transformed to one another by a simple scaling transformation (Figure 7b). Our finding that aligned textures were much more effective, despite these similarities, strongly constrains possible models of how perspective convergence is used.

The difference between aligned and perpendicular textures can be explained if perspective convergence is analyzed in terms of oriented spectral energy in local regions of the visual field. As described earlier (see Figure 3), an interesting property of the particular configurations of texture elements we used is that some of their symmetries

do not correspond to energy in their Fourier spectrum. In particular, the spectra of the perpendicular hex grid are missing energy in the horizontal direction. Although this texture is composed of clearly defined rows, the light and dark regions are balanced such that they “cancel” out when Fourier transformed, resulting in the absence of net energy at the spatial frequency of the rows. The absence of this component could account for why perspective convergence from this texture was less effective than from the aligned hex grid. Without considering the spectra, it would be hard to explain why rows in the perpendicular hex grid were so comparatively ineffective.

For the aligned hex grid, the absolute magnitude of thresholds implies that subjects could discriminate very fine differences in convergence. For a slant of 1.5 deg, which is

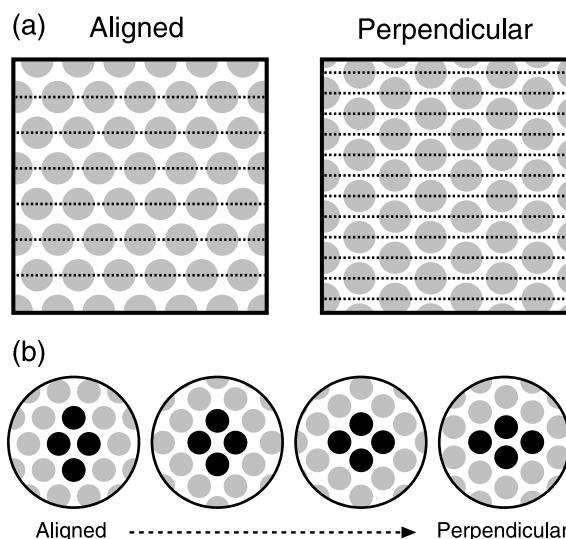


Figure 7. (a) Both aligned (left) and perpendicular (right) hex grid textures contain horizontal rows of elements, indicated by dotted lines. (b) The two position grids can be transformed to one another by scaling horizontal and vertical spacing, as illustrated in the bottom panels.

the lowest threshold we observed, the projected orientation of rows deviate from horizontal by only 0.4 deg at the top and bottom parts of the images. Orientation discrimination thresholds for line stimuli are generally observed to be higher, on the order of 1–3 deg (Heeley & Buchanan-Smith, 1998; Heeley, Buchanan-Smith, Cromwell, & Wright, 1997; Mareschal & Shapley, 2004; Orban, Vandenbussche, & Vogels, 1984; Regan & Price, 1986). The lower thresholds in our results suggest that there is spatial integration of local orientations across the image. This would be consistent with previous findings that orientation discrimination for lines improves with line length (Heeley & Buchanan-Smith, 1998; Orban et al., 1984).

## Experiment 2

In this experiment, we used another measure of the effectiveness of different texture types: the weighting of texture information relative to stereo information in binocular cue conflict stimuli. If texture and stereo information are optimally integrated, as found in other studies (Hillis et al., 2004; Knill & Saunders, 2003), one would expect that the relative weight given to texture would vary across texture types in predictable ways, with aligned textures being given more weight than perpendicular textures and isotropic textures being given less weight than either of these.

The same textures as in Experiment 1 were used, but the surfaces were presented binocularly, with stereo information specifying a slant that differed by  $\pm 5$  deg from the

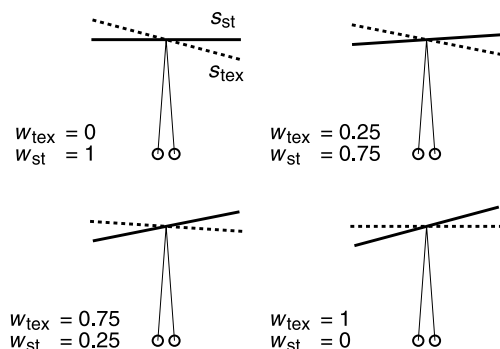


Figure 8. Illustration of how texture and stereo weights are related to the texture and stereo slants of a subjectively frontal cue conflict stimuli. Upper left: Perceived slant is determined by stereo information ( $w_{\text{tex}} = 0$ ). The conflict stimulus appears frontal when stereo slant cues indicate a frontal surface ( $S_{\text{st}} = 0$ ), regardless of texture slant. Bottom right: Perceived slant is determined by texture information ( $w_{\text{tex}} = 1$ ). The conflict stimulus appears frontal when the projected texture is uniform ( $S_{\text{tex}} = 0$ ), regardless of stereo slant. The other figures depict intermediate cases. For our results, we computed texture weights using the subjectively frontal stimuli for both positive and negative slant conflicts (see Appendix B).

slant specified by texture. The difference in PSE for these two conflict values was used to estimate the weight of texture relative to stereo (see Figure 8).

## Methods

### Apparatus and display

Experiment 2 used the same haploscope setup as in Experiment 1, but images were presented to both eyes rather than monocularly and were centered relative to the cyclopean eye rather than relative to the right eye. As before, the images depicted planar textured surfaces viewed through a blurred aperture. The binocular disparity of the aperture corresponded to a simulated viewing distance of 24 cm, whereas the textured surfaces had a simulated distance of 40 cm at their center. We used a relatively large separation between apertures and surface to prevent the relative disparity between surface and aperture from being a useful cue for the task. The region of the surface visible to both eyes subtended 16.6 deg horizontally, and the monocular flanking regions each subtended 13.3 deg horizontally.

The binocular images were constructed so that the slant indicated by texture information ( $s_{\text{tex}}$ ) differed from the slant specified by stereo information ( $s_{\text{st}}$ ) by  $\pm 5$  deg. These cue conflicts were generated by a double-projection method (e.g., Hillis et al., 2004; Knill & Saunders, 2003, after Banks & Backus, 1998). Surface texture was first projected from a slant  $s_{\text{tex}}$  onto an image plane relative to a cyclopean eye. Then, the result was back projected onto a surface with slant  $s_{\text{st}}$ , resulting in a slightly distorted pattern of texture along the stereo-specified surface. The final binocular images were the left and right eyes' accurate perspective views of this surface.

### Procedure

The four subjects were the same as in Experiment 1. Subjects performed four experimental sessions, each with a block of monocular stimuli (Experiment 1) and binocular stimuli (Experiment 2), in counterbalanced order. The binocular blocks each consisted of 360 trials, yielding a total of 480 trials per texture type condition, half with positive cue conflicts and half with negative conflicts. Texture type and sign of cue conflict were both randomized across trials in a block.

The task and procedure were the same as in Experiment 1: Stimuli were presented for 1 s, and subjects judged the direction of surface slant relative to frontal. The same adaptive procedure was used to select test slants, and PSEs and thresholds were estimated by maximum likelihood fits with a cumulative Gaussian as before.

Two additional analyses were performed for Experiment 2: (1) estimating the relative cue weights given to stereo and texture and (2) estimating the *predicted* relative cue weights, given subjects' discrimination thresholds, under the assumption of optimal integration. The details of these analyses are given in Appendix B.



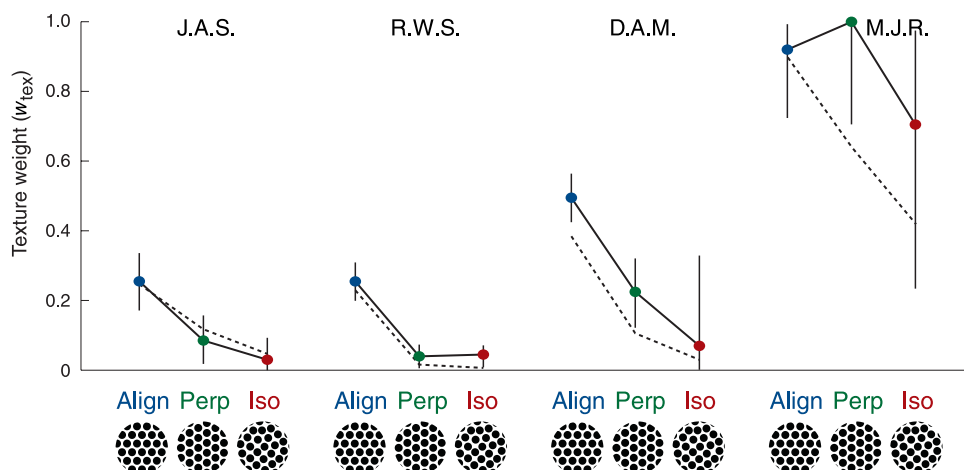


Figure 9. Measured (solid) and predicted (dashed) texture weights for each subject and texture type in [Experiment 2](#) (binocular stimuli). Error bars depict 95% confidence intervals. Texture weight was lowest for the isotropic texture and highest for the aligned hex grids as predicted from their reliabilities (as estimated from discrimination thresholds in [Experiments 1](#) and [2](#)—see text).

## Results and discussion

The solid lines in [Figure 9](#) plot the weights given to texture for the three texture types, as computed from the difference in PSEs for the positive and negative conflict conditions, for each of the four subjects. The dashed lines depict the predicted weights, given the subjects' discrimination performance for monocular and stereo conditions and assuming optimal integration. Overall, there was close agreement between observed and predicted weights. This indicates that the differences in texture weights are consistent with the differences in discrimination thresholds observed in the first experiment: Textures that produced lower thresholds were given greater weight relative to stereo information, consistent with the predictions of an optimal model. [Figure 10](#) plots observed versus predicted weights across subjects and conditions; most points are close to the diagonal.

One of the subjects, M.J.R., relied entirely on texture and gave no significant weight to stereo in any of the texture conditions. We consider this subject separately. The other subjects all gave nonzero weight to both texture and stereo in the cases of the aligned and perpendicular textures ( $p < .01$ ). Subject R.W.S. also gave nonzero weight to texture information provided by isotropic textures, whereas subjects J.A.S. and D.A.M. relied entirely on stereo information in this condition (J.A.S.:  $p = .14$ , *ns*; D.A.M.:  $p = .27$ , *ns*). For all subjects except M.J.R., there was a significant difference between the weight given to aligned grid texture and the weight given to either the isotropic texture or the perpendicular grid texture ( $p < .01$ ). The difference between the weights given to perpendicular textures and isotropic textures was not reliable for these subjects (J.A.S.:  $p = .12$ , *ns*; R.W.S.:  $p = .47$ , *ns*; D.A.M.:  $p = .17$ , *ns*). Given the low texture weights, this lack of difference could likely be a floor effect.

For subject M.J.R., stereo was not an effective cue for slant. This subject's threshold for stereo stimuli with isotropic textures was 20 deg, and based on his overall set of thresholds (monocular and binocular), we estimated his stereo-only threshold to be 24.5 deg. Thus, for this subject, [Experiment 2](#) was little different from [Experiment 1](#)—in both, responses were based primarily on monocular

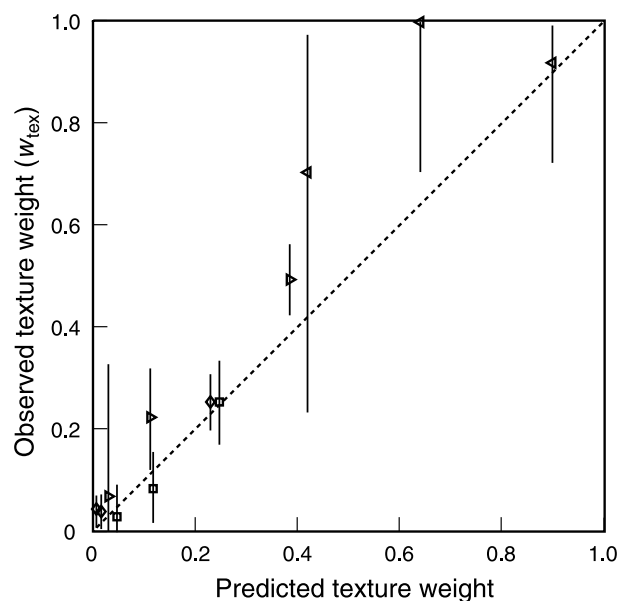


Figure 10. Data from [Figure 9](#) combined across subjects. The points plot observed texture weights as a function of the texture weight predicted from monocular and binocular discrimination performance. Different symbols correspond to the four subjects. Error bars show 95% confidence intervals (see text). The points lie close to the diagonal, indicating good agreement between observed and predicted weights.

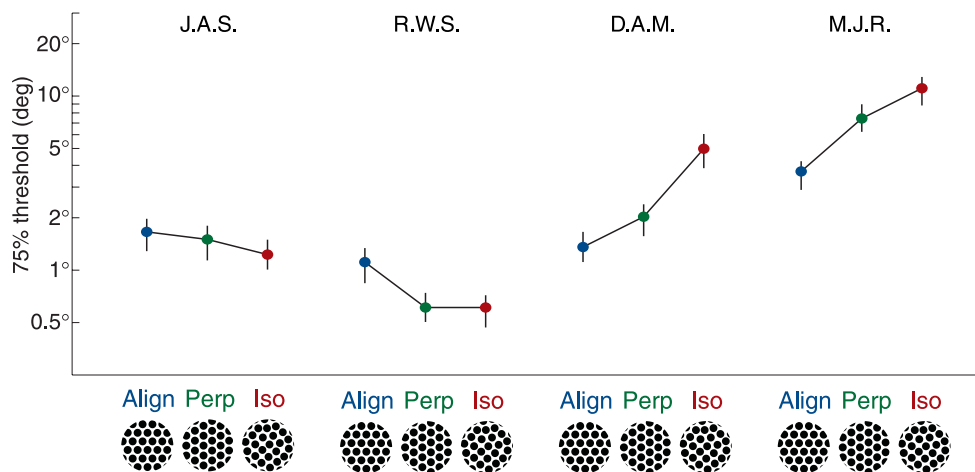


Figure 11. Seventy-five percent slant discrimination thresholds for binocular stimuli in [Experiment 2](#), for each subject and texture type. Error bars depict 95% confidence intervals.

information. Note that his data were still consistent with an optimal integration model, but the predictions are uninteresting: Relative texture weights were close to 1.0 across conditions.

[Figure 11](#) shows the discrimination thresholds for [Experiment 2](#). Not surprisingly, thresholds were reduced when additional information from stereo was available. The two subjects who relied on stereo the most (J.A.S. and R.W.S.) showed large improvements in thresholds relative to the monocular conditions tested in [Experiment 1](#). They no longer show an advantage for aligned textures over the other textures. Subject M.J.R. showed only modest improvements in thresholds relative to the monocular stimuli, and thresholds exhibited the same pattern of differences across texture types ( $p < .01$ ). Subject D.A.M. showed intermediate results: a clear improvement in thresholds with the addition of stereo, with residual differences across the texture types in the direction observed previously. Thus, the observed thresholds for the binocular stimuli were generally consistent with the observed cue weights.

The results of [Experiment 2](#) support the conclusion that perspective convergence contributes to perception of slant for surfaces near frontal. The presence of oriented symmetry in the texture arrangements not only improves slant discrimination performance, as demonstrated in [Experiment 1](#), but also causes texture to be given greater weight when integrated with slant information from stereo.

Previous studies have similarly found that surface textures have a greater influence on perceived slant relative to stereo information when they provide a perspective convergence cue. Allison and Howard (2000) and Gillam (1968) both tested cue conflict stimuli for which surface textures consisted of parallel dotted lines along a surface, with orientations either aligned or perpendicular to the direction of slant. Both studies found that the aligned textures, which produce convergence, had greater effect relative to conflicting stereo information. This is consistent with our finding of different cue weighting for aligned and perpendicular

textures. Banks and Backus (1998) tested the role of texture information in modulating an induced stereo slant bias and found that a texture composed of dots arranged in a grid had more effect than an isotropic texture composed of random dots. This is consistent with our finding of different weights for our aligned and isotropic textures, which similarly differ by whether their arrangement has oriented symmetry.

A possible concern about the task is that in [Experiment 1](#), stimuli could admit a 2D image-based strategy that was not based on perceived slant. Subjects could potentially have made veridical responses by judging the direction of convergence of the horizontal components, rather than based on the 3D slant that the convergence would imply. By this hypothesis, the subjects would essentially have been making 2D orientation judgments (change in 2D orientation across space) rather than 3D slant judgments. In the aligned hex condition, the symmetry lines were clearly salient; hence, a 2D strategy cannot be trivially dismissed. The results of [Experiment 2](#) partially address this concern. The results indicate that subjects were not relying exclusively on texture information, as would be predicted for an extreme version of a 2D strategy. Neither did subjects completely ignore texture information.

Because both texture and stereo information contributed to responses, it is tempting to assume that subjects' judgments were based on an integrated percept of slant, based on the combined information. Indeed, perceptual fusion has been explicitly demonstrated for the case of stereo and texture (Hillis, Ernst, Banks, & Landy, 2002). However, for two of the subjects (J.A.S. and R.W.S.), the size of the cue conflicts were well above the single-cue discrimination thresholds. These subjects could potentially have had perceptual access to individual cues, raising the possibility of some hybrid 2D/3D strategy. This could explain why the combined-cue thresholds for J.A.S. and R.W.S. showed a different pattern across texture types as compared to [Experiment 1](#). Alternatively, it could be that the fused percepts were less stable when cue conflicts were large compared to discrimination thresholds. Thus, we can conclude from [Experiment 2](#) that

texture information was used in the 3D slant task but not whether judgments were based on an integrated percept of slant. Subjects were instructed to indicate slant and were not given feedback; thus, for us, perceived slant seems to be the most likely basis for subjects' judgments.

## General discussion

### Role of perspective convergence

Our results show that when a surface texture contains an oriented symmetry, it is much easier to detect small slants relative to the frontal plane, as would be expected if perspective convergence contributed as a slant cue. Moreover, the greatest advantage was observed when an oriented symmetry was aligned with the direction of tilt—the alignment for which the perspective convergence is maximal. Textures were constructed to provide ideal information from local compression (all were projections of perfect circles) and from the gradient of size or average spatial frequency (all elements uniform in size). The only difference was in the arrangement of texture elements. For this reason, the stimuli provide a strong test of whether perspective convergence contributes to slant perception. The textures with perspective convergence were more effective at conveying slant as measured in two different ways. [Experiment 1](#) demonstrated that slant discrimination thresholds based on texture alone (monocular presentation) were lower for textures with oriented symmetries, and [Experiment 2](#) demonstrated that greater weight was given to texture information relative to stereo information for such textures in cue conflict situations. Both of these results are consistent with use of perspective convergence to perceive slant.

A recent study by Rosas et al. (2004) also measured slant discrimination thresholds for isotropic textures and textures that provided perspective convergence cues. Thresholds were measured around a range of base slants, as a way to quantify the effectiveness of various types of textures at various slants. There were clear differences between the classes of textures, particularly at the lower base slant of 20 deg, but overall, the differences were modest. In particular, they found that performance for a highly regular isotropic texture was as good or better than for grid or plaid textures that provide convergence. This appears to conflict with our results. However, although Rosas et al. tested conditions with a range of base slants, they did not include a condition in which surfaces varied around the frontal plane, as in our experiment. We suspect that performance in the experiment of Rosas et al. depended primarily on compression information and that if they had tested discrimination around the frontal plane, they would have observed a dramatic difference between textures with and without convergence information.

We focused on surfaces that have slants near zero—close to the frontal plane—because at low slants the information

provided by texture compression is poor (Knill, 1998a). If a surface texture is isotropic, convergence is also eliminated as a potential cue; thus, slant perception would have to be based on other texture cues such as the gradients of size and spacing. The isotropic textures we tested were not effective at conveying slant at low slants, despite their high uniformity in the size and spacing of texture elements; hence, size and spacing were not effective cues, consistent with Knill (1998b) and Knill and Saunders (2003).

If perspective convergence is the primary texture cue for slant when surfaces are near frontal, this could explain a discrepancy between the results of Knill and Saunders (2003) and those of Hillis et al. (2004). Despite similar paradigms, Hillis et al. observed much smaller thresholds than Knill and Saunders for surfaces near frontal: 8 deg versus 40 deg. Both studies used Voronoi textures with discrete elements. However, the textures used by Knill and Saunders were isotropic, generated by applying a diffusion process to randomly chosen initial positions, whereas the textures used by Hillis et al. were generated by randomly perturbing the positions of elements relative to an initial rectangular grid arrangement. These perturbed arrangements would have retained some of the oriented symmetry of the base grid. The present results suggest that this residual symmetry would have significantly improved discrimination performance in the case of slants around the frontal plane.

Previous studies have found that, when surfaces are more slanted, texture compression dominates perceived slant and that size and density cues are given comparatively little if any weight (Buckley et al., 1996; Knill, 1998c; Rosenholtz & Malik, 1997; Saunders, 2003). The present results, together with these earlier findings, support the general conclusion that size and density gradients are simply not very effective at eliciting perceived slant. There is some evidence that these cues have greater effect when field of view is increased (Todd et al., 2005), as might be expected for gradient-based cues. But clearly, an ideal observer designed to exploit size or density gradients would be expected to do much better at discriminating slant than our subjects did, for textures as regular and uniform as those tested here.

The models proposed by Malik and Rosenholtz (1997) and by Sakai and Finkel (1997) would be expected to perform well for the isotropic texture we used in our experiments. Our aligned and perpendicular hex grids provide virtually equivalent input from the standpoint of either of these models. Thus, these approaches do not appear to be representative of slant-from-texture analysis used by the human visual system.

### Oriented-energy model of slant from texture

Our results are consistent with a model that uses oriented components in local image spectra to compute slant from perspective convergence. Better slant discrimination for hex grids than isotropic textures is consistent with such a model because the isotropic textures do not provide any

perspective convergence cue. A stronger test comes from the comparison between the aligned and perpendicular hex grids. The perpendicular grid has horizontal symmetry and is very similar to the aligned grid but lacks spectral energy at the orientation and frequency corresponding to their horizontal rows. This difference was sufficient to dramatically impair discrimination performance, which strongly suggests that spectral components are the basis for the texture analysis.

Our results are in general agreement with those of Li and Zaidi (2000, 2001, 2003) and Zaidi and Li (2002), who similarly report that textures with discrete spectral energy components in the tilt direction were much more effective in conveying 3D shape than isotropic textures. On the other hand, our results do not support Li and Zaidi's (2000, 2001) stronger claim that oriented energy, within a narrow range around the tilt direction, is both necessary and sufficient. Performance was significantly worse for isotropic textures, but subjects could still make reliable judgments, with thresholds of 7–19 deg. A likely factor is the comparatively larger field of view used in our experiment (30 deg vs. 4 deg). Other counterexamples to the necessity condition have been presented (Todd & Oomes, 2002; Todd et al., 2004). Our results also contradict the sufficiency claim: The perpendicular texture in our experiment did have a discrete peak in their spectra, in the horizontal direction, but were clearly less effective than the aligned texture. Our discrimination task is likely a more sensitive measure than the qualitative tasks used by Li and Zaidi, which could explain the discrepancy.

The slant-from-texture models of Super and Bovik (1995) and Turner et al. (1991) assume that surfaces have a dominant overall orientation and spatial frequency and would therefore perform well for oriented textures but not for isotropic textures, consistent with our findings. On the other hand, because these models jointly fit spatial frequency and orientations, they would make effective use of the compression gradients in our hex grid textures and, therefore, would not predict the large difference between aligned and perpendicular textures.

The difference in effectiveness of aligned and perpendicular textures could be explained by a model based on oriented spectral components if one takes into account potential measurement error. Assuming noise in image orientation measurement, the reliability of a perspective convergence cue would depend on the amount of convergence. Oriented components aligned with the direction of tilt would therefore be most informative, and diagonally oriented components would be less informative. Consequently, the convergence information provided by the oriented component at 0 deg relative to the tilt direction, as in aligned textures, would be greater than the convergence information provided by oriented components at  $\pm 30$  deg, as in perpendicular textures.

The perpendicular texture contains high spatial frequency components that are aligned with the tilt direction, but these

components are evidently not very effective for eliciting perceived slant. We assume that these components are masked by the lowest spatial frequency components or that their contrast energy is too low to provide effective signals for the mechanisms that measure perspective convergence.

How would an oriented-energy model account for the difference between the perpendicular hex grid and the isotropic texture? The former enjoys at least three potential advantages over the latter. First, the perpendicular hex grid has energy in the horizontal direction at higher frequencies. Second, the perspective convergence of diagonal components ( $\pm 30$  deg relative to horizontal) could contribute. Third, the perpendicular hex grid might effectively produce some “energy” in the horizontal direction at the base frequency due to some nonlinearity in the initial processing of texture, as suggested by Li and Zaidi (see Figure 19 of Li & Zaidi, 2000). Our results do not distinguish these possibilities, and it is possible that any or all of these factors could contribute.

## Conclusion

We have shown that the presence of oriented symmetries can greatly increase the effectiveness of texture as a cue for the slant of surfaces that are close to frontal, even when other texture cues (size, shape, and spacing) provide nearly ideal information. At higher slants, other studies have found compression to be the primary texture cue. Our results show that, when surfaces are nearly frontal, perspective convergence becomes the primary factor when available and has greater influence on perceived slant than the combined contributions of size, density, or other gradient texture cues. Our results further suggest that the use of perspective convergence is based on oriented spectral contrast energy and that textures with spectral components that are aligned with the direction of surface slant are the most effective at conveying slant.

## Appendix A: Minimized expected entropy staircase method

In selecting the slant values to test on each trial, we used a newly developed adaptive procedure, which we term the *minimized expected entropy* method. For a given trial, the probe slants and responses from previous trials in the same condition,  $\{s_k, r_k\}$ , were used to estimate a posterior probability distribution  $P(\mu, \sigma | s_1, r_1, s_2, r_2, \dots, s_n, r_n)$ , where  $\mu$  is the PSE and  $\sigma$  is the difference between the PSE and the 75% point. The next probe  $s_{n+1}$  was chosen to minimize the expected entropy,  $-p \log(p)$ , of the posttrial posterior function,  $P(\mu, \sigma | s_1, r_1, s_2, r_2, \dots, s_{n+1}, r_{n+1})$ . The entropy cost function rewards probes that would be expected to result in a

more peaked and concentrated posterior distribution over the space of possible combinations of  $\mu$  and  $\sigma$ , consistent with the goal of estimating  $\mu$  and  $\sigma$  with minimal bounds of uncertainty. There are only two possibilities for the next response, 0 or 1, and for each of these possibilities, one can compute what the new postresponse likelihood distribution would be, as well as its entropy. The expected value of entropy is simply a weighted average of the two possible results, where weights are proportional to their probabilities,  $P(r_{n+1} = 0|s_{n+1})$  and  $P(r_{n+1} = 1|s_{n+1})$ . If  $\mu$  and  $\sigma$  were known, these probabilities would be directly determined by the model psychometric function. Thus, to estimate  $P(r_{n+1}|s_{n+1})$ , we marginalized over  $\mu$  and  $\sigma$ , using the posterior distribution computed from previous response history as an estimate of  $P(\mu, \sigma)$ :

$$P(r_{n+1}|s_{n+1}) \approx \sum_{\mu, \sigma} P(r_{n+1}|s_{n+1}, \mu, \sigma) \cdot P(\mu, \sigma | s_1, r_1, \dots, s_n, r_n). \quad (\text{A1})$$

For probe slant selection, we used a logistic function to model the psychometric function  $P(r_{n+1}|s_{n+1}, \mu, \sigma)$ , rather than a more standard cumulative Gaussian, to simplify computation. The function was scaled to range from 0.025 to 0.975 rather than from 0 to 1, to reduce the effect of lapses of attention and guessing on the probe selection. Informal testing of the procedure revealed it to be highly efficient and robust. The space of possible bias and threshold values was discretely sampled to carry out the marginalization, with  $\mu$  sampled linearly from  $-30$  and  $30$  deg and with  $\sigma$  sampled quadratically from 0.25 to 36.

We have not compared its efficiency to other Bayesian psychometric procedures such as QUEST (Watson & Pelli, 1983).

## Appendix B: Measurement and prediction of cue weights

To compute cue weights, we assumed a linear model of cue combination: perceived slant  $S_{\text{per}}$  is a weighted average of the slants estimated from stereo information,  $S_{\text{ster}}$ , and from texture information,  $S_{\text{tex}}$ :

$$S_{\text{per}} = S_{\text{tex}} \cdot w_{\text{tex}} + S_{\text{st}} \cdot w_{\text{st}}. \quad (\text{B1})$$

The case where  $S_{\text{per}} = 0$  corresponds to the situation where stereo and texture information null each other, such that the perceived orientation from the combined slant information appears frontal. As illustrated in Figure 8, the combination of  $S_{\text{tex}}$  and  $S_{\text{st}}$  that produces a frontal percept is related to the relative magnitude of stereo and texture weights.

We assumed that the cue weights  $w_{\text{tex}}$  and  $w_{\text{st}}$  sum to 1. This corresponds to ignoring the potential contributions from slant cues other than stereo or texture, such as accommodation. However, any such slant cues would be consistent with frontal plane—the orientation of the display monitors—and, therefore, would not be expected to affect what combination of texture and stereo cues null each other (Backus, Banks, van Ee, & Crowell, 1999).

Across trials in a condition, the slant specified by texture and slant differed by a constant amount,  $S_{\text{tex}} = S_{\text{st}} + \Delta S$ , where  $\Delta S$  on each trial was  $\pm 5$  deg. Perceived slant can therefore be expressed as:

$$S_{\text{per}} = S_{\text{st}} + \Delta S \cdot w_{\text{tex}}. \quad (\text{B2})$$

We fit PSEs and thresholds as functions of stereo slant  $S_{\text{st}}$  in the same manner as in Experiment 1. As there could be systematic bias in an observer's internal standard for frontal, we did not interpret PSEs as a direct measure of where  $S_{\text{per}} = 0$ . Rather, we combined PSEs for positive and negative conflict stimuli to compute texture weights:

$$w_{\text{tex}} = (S_{\text{st}}^- - S_{\text{st}}^+) / (2 \cdot |\Delta S|), \quad (\text{B3})$$

where  $S_{\text{st}}^+$  and  $S_{\text{st}}^-$  are the stereo slants that null perceived slant for  $\Delta S > 0$  and  $\Delta S < 0$ , respectively (see, e.g., Backus & Matza-Brown, 2003).

We also computed the weights that would be predicted from subjects' discrimination thresholds, assuming optimal integration. If measurement noise in the perceptual estimates of  $S_{\text{tex}}$  and  $S_{\text{st}}$  is assumed to be Gaussian, then the optimal Bayesian estimate of slant can be described as a weighted sum, as in Equation B1, with weights being inversely proportional to the variances of the noise (see Knill & Saunders, 2003):

$$w_{\text{tex}} \sim 1/\sigma_{\text{tex}}^2, \quad w_{\text{st}} \sim 1/\sigma_{\text{st}}^2. \quad (\text{B4})$$

To compute predicted weights for optimal integration, we further assumed that subjects' discrimination performance was primarily limited by sensory measurement noise and that other sources of variability like decision noise were negligible. In this case, the discrimination thresholds observed for single-cue stimuli,  $T_{\text{tex}}$  and  $T_{\text{st}}$ , can be taken as representing the standard deviations of the single-cue measurement noise,  $\sigma_{\text{tex}}$  and  $\sigma_{\text{st}}$ :

$$w_{\text{tex}} \sim 1/T_{\text{tex}}^2, \quad w_{\text{st}} \sim 1/T_{\text{st}}^2. \quad (\text{B5})$$

The thresholds obtained in Experiment 1 provide measures of slant discrimination ability based on texture information only,  $T_{\text{tex}}$ , for the various texture types. However, we did not measure slant discrimination for stimuli that provide only stereo information, as was done in Knill and

Saunders (2003) and Hillis et al. (2004). Instead, we inferred a stereo discrimination threshold  $T_{st}$  for each subject, based on the combined-cue discrimination thresholds observed in Experiment 2. If stereo and texture information are optimally integrated in a linear model (i.e., weights satisfy Equation B4) and if performance is limited primarily by sensory noise, then the thresholds for combined-cue stimuli can be predicted based on the thresholds for single-cue stimuli:

$$1/T_{st+tex}^2 \approx 1/T_{tex}^2 + 1/T_{st}^2. \quad (B6)$$

The thresholds measured for the binocular stimuli in Experiment 2 provide estimates of  $T_{st+tex}$  for each of the three texture types. We inferred the stereo-only threshold for a subject,  $T_{st}$ , to be that which minimizes the sum squared error between the observed thresholds  $T_{st+tex}$  and the thresholds predicted by Equation B6 using the single-cue thresholds from Experiment 1 as  $T_{tex}$ . We then used this inferred stereo threshold,  $T_{st}$ , together with the texture-only thresholds,  $T_{tex}$ , for each texture condition to compute predicted texture cue weights,  $w_{tex}$ , from Equation B5.

## Acknowledgments

This research was supported by NIH Grant EY-013988.

Commercial relationships: none.

Corresponding author: Jeffrey A. Saunders.

Email: jeffrey\_a\_saunders@yahoo.com.

Address: 3401 Walnut Street, Philadelphia, PA 19104, USA.

## Footnote

<sup>1</sup>A single set of convergent symmetry lines does not fully specify the 3D orientation of the surface but rather constrains slant and tilt to a one-parameter subset within the space of possible slant and tilt combinations. Some additional information would be required to uniquely determine both slant and tilt, such as gradients of size or spacing or the perspective convergence of another set of symmetry lines (if the surface has multiple-oriented symmetries).

## References

- Allison, R. S., & Howard, I. P. (2000). Temporal dependencies in resolving monocular and binocular cue conflict in slant perception. *Vision Research*, *40*, 1869–1885. [PubMed]
- Aloimonos, J., & Swain, M. (1988). Shape from patterns—Regularization. *International Journal of Computer Vision*, *2*, 171–187.
- Andersen, G. J., Braunstein, M. L., & Saidpour, A. (1998). The perception of depth and slant from texture in three-dimensional scenes. *Perception*, *27*, 1087–1106. [PubMed]
- Backus, B. T., Banks, M. S., van Ee, R., & Crowell, J. A. (1999). Horizontal and vertical disparity, eye position, and stereoscopic slant perception. *Vision Research*, *39*, 1143–1170. [PubMed]
- Backus, B. T., & Matza-Brown, D. (2003). The contribution of vergence change to the measurement of relative disparity. *Journal of Vision*, *3*(11), 737–750, <http://journalofvision.org/3/11/8/>, doi:10.1167/3.11.8. [PubMed] [Article]
- Banks, M. S., & Backus, B. T. (1998). Extra-retinal and perspective cues cause the small range of the induced effect. *Vision Research*, *38*, 187–194. [PubMed]
- Beck, J. (1960). Texture-gradients and judgments of slant and recession. *American Journal of Psychology*, *73*, 411–416. [PubMed]
- Blake, A., Bulthoff, H. H., & Sheinberg, D. (1993). Shape from texture: Ideal observers and human psychophysics. *Vision Research*, *33*, 1723–1737. [PubMed]
- Blostein, D., & Ahuja, N. (1989). Shape from texture: Integrating texture-element extraction and surface estimation. *IEEE Transactions on Pattern Analysis and Machine Intelligence*, *11*, 1233–1251.
- Braunstein, M. L., & Payne, J. W. (1969). Perspective and form ratio as determinants of relative slant judgments. *Journal of Experimental Psychology*, *81*, 584–590.
- Buckley, D., Frisby, J. P., & Blake, A. (1996). Does the human visual system implement an ideal observer theory of slant from texture? *Vision Research*, *36*, 1163–1176. [PubMed]
- Cumming, B. G., Johnston, E. B., & Parker, A. J. (1993). Effects of different texture cues on curved surfaces viewed stereoscopically. *Vision Research*, *33*, 827–838. [PubMed]
- Cutting, J. E., & Millard, R. T. (1984). Three gradients and the perception of flat and curve surfaces. *Journal of Experimental Psychology*, *113*, 198–216. [PubMed]
- Gårding, J. (1993). Shape from texture and contour by weak isotropy. *Artificial Intelligence*, *64*, 243–297.
- Gibson, J. J. (1950). *The perception of the visual world*. Boston: Houghton Mifflin.
- Gillam, B. J. (1968). Perception of slant when perspective and stereopsis conflict: Experiments with aniseikonic lenses. *Journal of Experimental Psychology*, *78*, 299–305. [PubMed]

- Heeley, D. W., & Buchanan-Smith, H. M. (1998). The influence of stimulus shape on orientation acuity. *Experimental Brain Research*, *120*, 217–222. [PubMed]
- Heeley, D. W., Buchanan-Smith, H. M., Cromwell, J. A., & Wright, J. S. (1997). The oblique effect in orientation acuity. *Vision Research*, *37*, 235–242. [PubMed]
- Hillis, J. M., Ernst, M. O., Banks, M. S., & Landy, M. S. (2002). Combining sensory information: Mandatory fusion within, but not between, sense. *Science*, *298*, 1627–1630. [PubMed]
- Hillis, J. M., Watt, S. J., Landy, M. S., & Banks, M. S. (2004). Slant from texture and disparity cues: Optimal cue combination. *Journal of Vision*, *4*(12), 967–992. <http://journalofvision.org/4/12/1/>, doi:10.1167/4.12.1. [PubMed] [Article]
- Ikeuchi, K. (1984). Shape from regular patterns. *Artificial Intelligence*, *22*, 49–75.
- Knill, D. C. (1998a). Discrimination of planar surface slant from texture: Human and ideal observers compared. *Vision Research*, *38*, 1683–1711. [PubMed]
- Knill, D. C. (1998b). Ideal observer perturbation analysis reveals human strategies for inferring surface orientation from texture. *Vision Research*, *38*, 2635–2656. [PubMed]
- Knill, D. C. (1998c). Surface orientation from texture: Ideal observers, generic observers and the information content of texture cues. *Vision Research*, *38*, 1655–1682. [PubMed]
- Knill, D. C. (2001). Contour into texture: Information content of surface contours and texture flow. *Journal of the Optical Society of America A, Optics, Image Science, and Vision*, *18*, 12–35. [PubMed]
- Knill, D. C., & Saunders, J. A. (2003). Do humans optimally integrate stereo and texture information for judgments of surface slant? *Vision Research*, *43*, 2539–2558. [PubMed]
- Li, A., & Zaidi, Q. (2000). Perception of three-dimensional shape from texture is based on patterns of oriented energy. *Vision Research*, *40*, 217–242. [PubMed]
- Li, A., & Zaidi, Q. (2001). Information limitations in perception of shape from texture. *Vision Research*, *41*, 1519–1533. [PubMed]
- Li, A., & Zaidi, Q. (2003). Observer strategies in perception of 3-D shape from isotropic textures: Developable surfaces. *Vision Research*, *43*, 2741–2758. [PubMed]
- Li, A., & Zaidi, Q. (2004). Three-dimensional shape from non-homogeneous textures: Carved and stretched surfaces. *Journal of Vision*, *4*(10), 860–878. <http://journalofvision.org/4/10/3/>, doi:10.1167/4.10.3. [PubMed] [Article]
- Malik, J., & Rosenholtz, R. (1997). Computing local surface orientation and shape from texture for curved surfaces. *International Journal of Computer Vision*, *23*, 149–168.
- Mareschal, I., & Shapley, R. M. (2004). Effects of contrast and size on orientation discrimination. *Vision Research*, *44*, 57–67. [PubMed]
- Orban, G. A., Vandebussche, E., & Vogels, R. (1984). Human orientation discrimination tested with long stimuli. *Vision Research*, *24*, 121–128. [PubMed]
- Passmore, P. J., & Johnston, A. (1995). Human discrimination of surface slant in fractal and related textured images. *Spatial Vision*, *9*, 151–161. [PubMed]
- Regan, D., & Price, P. (1986). Periodicity in orientation discrimination and the unconfounding of visual information. *Vision Research*, *26*, 1299–1302. [PubMed]
- Rosas, P., Wichmann, F. A., & Wagemans, J. (2004). Some observations on the effects of slant and texture type on slant-from-texture. *Vision Research*, *44*, 1511–1535. [PubMed]
- Rosenholtz, R., & Malik, J. (1997). Surface orientation from texture: Isotropy or homogeneity (or both)? *Vision Research*, *37*, 2283–2293. [PubMed]
- Sakai, K., & Finkel, L. H. (1995). Characterization of the spatial-frequency spectrum in the perception of shape from texture. *Journal of the Optical Society of America A, Optics, Image Science, and Vision*, *12*, 1208–1224. [PubMed]
- Sakai, K., & Finkel, L. H. (1997). Spatial-frequency analysis in the perception of perspective depth. *Network*, *8*, 335–352.
- Saunders, J. A. (2003). The effect of texture relief on perception of slant from texture. *Perception*, *32*, 211–233. [PubMed]
- Saunders, J. A., & Knill, D. C. (2001). Perception of 3D surface orientation from skew symmetry. *Vision Research*, *41*, 3163–3183. [PubMed]
- Stevens, K. A. (1981a). The information content of texture gradients. *Biological Cybernetics*, *42*, 95–105. [PubMed]
- Stevens, K. A. (1981b). The visual interpretation of surface contours. *Biological Cybernetics*, *42*, 47–53.
- Super, B. J., & Bovik, A. C. (1995). Planar surface orientation from texture spatial-frequencies. *Pattern Recognition*, *28*, 729–743.
- Tibau, S., Willems, B., Van den Bergh, E., & Wagemans, J. (2001). The role of the centre of projection in the estimation of slant from texture of planar surfaces. *Perception*, *30*, 185–193. [PubMed]
- Todd, J. T., & Akerstrom, R. A. (1987). Perception of three-dimensional form from patterns of optical texture. *Journal of Experimental Psychology: Human Perception and Performance*, *13*, 242–255. [PubMed]

- Todd, J. T., & Oomes, A. H. (2002). Generic and non-generic conditions for the perception of surface shape from texture. *Vision Research*, *42*, 837–850. [[PubMed](#)]
- Todd, J. T., Oomes, A. H., Koenderink, J. J., & Kappers, A. M. (2004). The perception of doubly curved surfaces from anisotropic textures. *Psychological Science*, *15*, 40–46. [[PubMed](#)]
- Todd, J. T., & Reichel, F. D. (1990). Visual perception of smoothly curved surfaces from double-projected contour patterns. *Journal of Experimental Psychology: Human Perception and Performance*, *16*, 665–674. [[PubMed](#)]
- Todd, J. T., Thaler, L., & Dijkstra, T. M. (2005). The effects of field of view on the perception of 3D slant from texture. *Vision Research*, *45*, 1501–1517. [[PubMed](#)]
- Turner, M. R., Gerstein, G. L., & Bajcsy, R. (1991). Underestimation of visual texture slant by human observers: A model. *Biological Cybernetics*, *65*, 215–226. [[PubMed](#)]
- Watson, A. B., & Ahumada, A. J., Jr. (2005). A standard model for foveal detection of spatial contrast. *Journal of Vision*, *5*(9), 717–740, <http://journalofvision.org/5/9/6/>, doi:10.1167/5.9.6. [[PubMed](#)] [[Article](#)]
- Watson, A. B., & Pelli, D. G. (1983). QUEST: A Bayesian adaptive psychometric method. *Perception & Psychophysics*, *33*, 113–120. [[PubMed](#)]
- Witkin, A. P. (1981). Recovering surface shape and orientation from texture. *Artificial Intelligence*, *17*, 17–45.
- Zaidi, Q., & Li, A. (2002). Limitations on shape information provided by texture cues. *Vision Research*, *42*, 815–835. [[PubMed](#)]